

## The influence of V/III ratio on electron mobility of the $\text{InAs}_x\text{Sb}_{1-x}$ layers grown on GaAs substrate by molecular beam epitaxy

ZHANG Jing<sup>1\*</sup>, YANG Zhi<sup>1</sup>, ZHENG Li-Ming<sup>2</sup>, ZHU Xiao-Juan<sup>1</sup>, WANG Ping<sup>1</sup>, YANG Lin<sup>3</sup>

- (1. School of Electronic Information and Artificial Intelligence, Shaanxi University of Science and Technology, Xi'an 710016, China;  
2. School of Mechanical and Electrical Engineering, Xi'an Traffic Engineering Institute, Xi'an 710300, China;  
3. School of Information Science and Engineering, Hebei University of Science and Technology, Shijiazhuang 050018, China)

**Abstract:** This paper discusses the influence of Sb/In ratio on the transport properties and crystal quality of the 200 nm  $\text{InAs}_x\text{Sb}_{1-x}$  thin film. The Sb content of  $\text{InAs}_x\text{Sb}_{1-x}$  thin film in all samples was verified by HRXRD of the symmetrical 004 reflections and asymmetrical 115 reflections. The calculation results show that the Sb component was 0.6 in the  $\text{InAs}_x\text{Sb}_{1-x}$  thin film grown under the conditions of Sb/In ratio of 6 and As/In ratio of 3, which has the highest electron mobility ( $28\,560\text{ cm}^2/\text{V}\cdot\text{s}$ ) at 300 K. At the same time, the influence of V/III ratio on the transport properties and crystal quality of  $\text{Al}_{0.2}\text{In}_{0.8}\text{Sb}/\text{InAs}_x\text{Sb}_{1-x}$  quantum well heterostructures also has been investigated. As a result, the  $\text{Al}_{0.2}\text{In}_{0.8}\text{Sb}/\text{InAs}_{0.4}\text{Sb}_{0.6}$  quantum well heterostructure with a channel thickness of 30 nm grown under the conditions of Sb/In ratio of 6 and As/In ratio of 3 has a maximum electron mobility of  $28\,300\text{ cm}^2/\text{V}\cdot\text{s}$  and a minimum RMS roughness of 0.68 nm. Through optimizing the growth conditions, our samples have higher electron mobility and smoother surface morphology.

**Key words:** molecular beam epitaxy,  $\text{InAs}_x\text{Sb}_{1-x}$ , V/III ratio, high electron mobility

## V/III 比对分子束外延生长的 GaAs 基 $\text{InAs}_x\text{Sb}_{1-x}$ 电子迁移率的影响

张静<sup>1\*</sup>, 阳智<sup>1</sup>, 郑黎明<sup>2</sup>, 朱小娟<sup>1</sup>, 王萍<sup>1</sup>, 杨琳<sup>3</sup>

- (1. 陕西科技大学 电子信息与人工智能学院, 陕西 西安 710016;  
2. 西安交通工程学院 机电工程学院, 陕西 西安 710300;  
3. 河北科技大学 信息科学与工程学院, 河北 石家庄 050018)

**摘要:** 研究了 Sb/In 比对 200 nm  $\text{InAs}_x\text{Sb}_{1-x}$  薄膜传输特性和晶体质量的影响。通过对称(004)扫描和非对称(115)扫描的 HRXRD 计算了所有样品中  $\text{InAs}_x\text{Sb}_{1-x}$  薄膜的 Sb 含量。计算结果表明, 在 Sb/In 比为 6 和 As/In 比为 3 的条件下生长的  $\text{InAs}_x\text{Sb}_{1-x}$  薄膜中, Sb 组分为 0.6。在  $\text{InAs}_x\text{Sb}_{1-x}$  薄膜在室温下测得的最高电子迁移率为  $28\,560\text{ cm}^2/\text{V}\cdot\text{s}$ 。同时, 本文还研究了 Sb/In 比和 As/In 比对  $\text{Al}_{0.2}\text{In}_{0.8}\text{Sb}/\text{InAs}_x\text{Sb}_{1-x}$  量子阱异质结的输运性质和晶体质量的影响。结果显示, 在 Sb/In 比为 6 和 As/In 比为 3 的条件下生长的沟道厚度为 30 nm 的  $\text{Al}_{0.2}\text{In}_{0.8}\text{Sb}/\text{InAs}_{0.4}\text{Sb}_{0.6}$  量子阱异质结的最高电子迁移率为  $28\,300\text{ cm}^2/\text{V}\cdot\text{s}$ , 最小表面粗糙度为 0.68 nm。通过优化生长条件, 我们的样品具有更好的晶体质量和更光滑的表面形貌。

**关键词:** 分子束外延;  $\text{InAs}_x\text{Sb}_{1-x}$ ; V/III 比; 高电子迁移率

中图分类号: TN304.2; TN305

文献标识码: A

Received date: 2024-01-20, revised date: 2024-06-19

收稿日期: 2024-01-20, 修回日期: 2024-06-19

**Foundation items:** Supported by the Natural Science Basic Research Program of Shaanxi Province (2023-JC-QN-0758), Shaanxi University of Science and Technology Research Launch Project (2020BJ-26), Doctoral Research Initializing Fund of Hebei University of Science and Technology, China (1181476).

**Biography:** Zhang Jing (1988—), female, Xi'an, China, lecturer. Research area involves semiconductor materials and devices. E-mail: zhangjing6048@sust.edu.cn

\*Corresponding author: E-mail: zhangjing6048@126.com

## Introduction

High-speed devices using III-V compound materials have become one of the international research hot-spots<sup>[1,2]</sup>. The narrow band-gap materials of InAs, InSb and InAsSb in III-V compounds not only have high electron mobility and electron saturation drift velocity, but also can form diverse quantum well band structures with AlSb, GaSb and other related ternary broadband gap materials<sup>[3-7]</sup>. These excellent characteristics allow the electrical devices to have the advantages of ultra-high speed and low power consumption. There has been some literature<sup>[8-10]</sup> on using InAs materials as channel layers to prepare high electron mobility transistor (HEMT). To pursue higher working speed and lower power consumption, the highest electron mobility in all III-V binary compounds of InSb has generated considerable interest for the fabrication of HEMT<sup>[11,12]</sup>. However, the growth of high-quality InSb is challenging due to the large lattice mismatch between InSb and GaAs substrates. To minimize the problem of lattice strain and improve mobility, InAsSb ternary alloy is anticipated to substitute of InSb and InAs. Meanwhile, the straddle energy band structure of  $\text{Al}_{0.2}\text{In}_{0.8}\text{Sb}/\text{InAs}_{0.4}\text{Sb}_{0.6}$  heterostructure is used to replace the interleaved energy band structure of InAs/AlSb heterostructure, which can effectively reduce the lattice mismatch and the gate leakage current caused by holes. Therefore, InAsSb material is expected to become a strong competitor as a channel material in the next generation of HEMT<sup>[13,14]</sup>.

Since the InAsSb material contains two V elements of As and Sb, the composition of group V elements cannot be accurately calculated by the ratio of growth rates. More influencing factors need to be considered when growing InAsSb materials because the adhesion of As and Sb elements varies under different growth conditions. Therefore, it is necessary to study the composition control of InAsSb materials grown by molecular beam epitaxy. Based on the theoretical calculation results reported in the current literature<sup>[15-17]</sup>, the electron mobility of InAsSb as a channel material can reach more than  $30\,000\text{ cm}^2/\text{V}\cdot\text{s}$ . However, the current experimental results are far lower than the simulation results due to challenges in the growth process such as interface mismatch and dislocation scattering<sup>[18-20]</sup>. In comparison, fewer reports on experimental results on the transport characteristics of the  $\text{InAs}_x\text{Sb}_{1-x}$  with different Sb content are available currently.

This paper discusses the influence of Sb/In ratio on the transport properties and crystal quality of the 200 nm  $\text{InAs}_x\text{Sb}_{1-x}$  thin film. The Sb content of  $\text{InAs}_x\text{Sb}_{1-x}$  thin film in all samples was verified by HRXRD via the symmetrical 004 reflections and asymmetrical 115 reflections. In addition, the influence of Sb/In ratio and As/In ratio on the transport properties and crystal quality of  $\text{Al}_{0.2}\text{In}_{0.8}\text{Sb}/\text{InAs}_x\text{Sb}_{1-x}$  quantum well heterostructures has also been investigated. By optimizing the Sb/In ratio and As/In ratio,  $\text{Al}_{0.2}\text{In}_{0.8}\text{Sb}/\text{InAs}_x\text{Sb}_{1-x}$  quantum well heterostructures with good surface morphology and high electron mobility were obtained. All samples were confirmed by atomic force microscopy (AFM), high-resolution X-ray diffraction

(HRXRD), reciprocal space map (RSM) and Hall measurement.

## 1 Experimental procedures

All samples were grown on GaAs substrate by Gen-II solid-source MBE system. After deoxidation of GaAs substrate at  $690\text{ }^\circ\text{C}$  for 5 minutes, a 100 nm GaAs was grown at  $650\text{ }^\circ\text{C}$  and a 100 nm GaSb was grown at  $540\text{ }^\circ\text{C}$  to ensure that the substrate surface was flat. For one structure, a  $1.5\text{ }\mu\text{m}$   $\text{Al}_{0.2}\text{In}_{0.8}\text{Sb}$  metamorphic buffer layer was used to study the transport properties of the 200 nm  $\text{InAs}_x\text{Sb}_{1-x}$  layer, as shown in Fig. 1. The 200 nm  $\text{InAs}_x\text{Sb}_{1-x}$  thin films of the first group of samples A1, A2 and A3 were grown at different the Sb/In ratios of 5, 6 and 7, while the As/In ratio is kept at about 3.

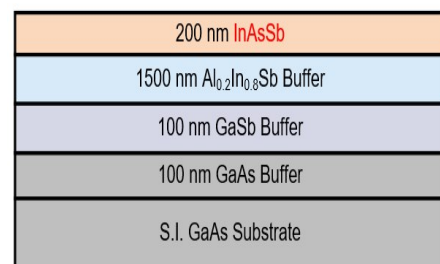


Fig. 1 Schematic diagram of  $\text{InAs}_x\text{Sb}_{1-x}$  thin film structure  
图1  $\text{InAs}_x\text{Sb}_{1-x}$ 薄膜结构示意图

For another structure, the  $\text{Al}_{0.2}\text{In}_{0.8}\text{Sb}/\text{InAs}_x\text{Sb}_{1-x}$  quantum well heterostructures were grown for preparing high electron mobility transistors, as shown in Fig. 2. For the  $\text{Al}_{0.2}\text{In}_{0.8}\text{Sb}/\text{InAs}_x\text{Sb}_{1-x}$  quantum well heterostructures, the  $1.5\text{ }\mu\text{m}$   $\text{Al}_{0.2}\text{In}_{0.8}\text{Sb}$  that acted as a lower barrier layer and buffer was directly deposited on the GaSb buffer layer. Then a different thicknesses  $\text{InAs}_x\text{Sb}_{1-x}$  channel, a 20 nm  $\text{Al}_{0.2}\text{In}_{0.8}\text{Sb}$  upper barrier layer and a 5 nm InSb cap layer were deposited on the top of the  $\text{Al}_{0.2}\text{In}_{0.8}\text{Sb}$  layer.



Fig. 2 Schematic diagram of  $\text{Al}_{0.2}\text{In}_{0.8}\text{Sb}/\text{InAs}_x\text{Sb}_{1-x}$  quantum well heterostructures  
图2  $\text{Al}_{0.2}\text{In}_{0.8}\text{Sb}/\text{InAs}_x\text{Sb}_{1-x}$ 量子阱异质结构示意图

The first group of samples B1, B2, and B3 with different Sb/In ratios (5, 6, 7) were grown to investigate the effects of different Sb components on the crystal quality and electron mobility of  $\text{Al}_{0.2}\text{In}_{0.8}\text{Sb}/\text{InAs}_x\text{Sb}_{1-x}$  quantum well heterostructures, while the As/In ratio was also kept

at about 3. Meanwhile, the channel thickness of this group of samples was 15 nm. The second group of samples C1, C2, and C3 with different As/In ratios (1, 2, 3) were grown to investigate the effects of different As components on the crystal quality and electron mobility of  $\text{Al}_{0.2}\text{In}_{0.8}\text{Sb}/\text{InAs}_x\text{Sb}_{1-x}$  quantum well heterostructures, while the Sb/In ratio was kept at about 6. Meanwhile, the channel thickness of this group of samples was increased from 15 nm to 30 nm. The third group of samples D1, D2, D3, D4 and D5 corresponds to  $\text{InAs}_{0.4}\text{Sb}_{0.6}$  channel layer thicknesses of 15, 20, 25, 30 and 35 nm to investigate the effect of different channel thicknesses on the crystal quality and electron mobility of  $\text{Al}_{0.2}\text{In}_{0.8}\text{Sb}/\text{InAs}_x\text{Sb}_{1-x}$  quantum well heterostructures. The Sb/In ratio was kept at about 6 and the As/In ratio was kept at about 3.

## 2 Results and discussion

### 2.1 The influences of Sb/In ratios on $\text{InAs}_x\text{Sb}_{1-x}$ thin films

Figure 3 displays  $2 \times 2 \mu\text{m}^2$  AFM images of samples A1, A2 and A3 with an RMS roughness of 0.287 nm, 0.28 nm and 0.6 nm, respectively. Atomic steps can be clearly seen in samples A2 and A3, indicating that the surfaces of the samples are very flat. However, some bright spots can be seen in sample A3. These were due to the excess Sb beam while the Sb/In ratio was 7, resulting in residual Sb elements on the surface. The  $10 \times 10 \mu\text{m}^2$  AFM images of samples A1, A2 and A3 can also be found that sample A2 has the smallest RMS value of

0.7 nm, which is much smaller than a recent literature report (1.9 nm)<sup>[21]</sup>.

The Sb content of the  $\text{InAs}_x\text{Sb}_{1-x}$  layer in all samples was verified by HRXRD via the symmetrical 004 reflections and asymmetrical 115 reflections, as shown in Fig. 4(a) and 4(b). The calculation results are shown in Table 1. The Sb composition of sample A1 was calculated to be 0.68 and the lattice constant of  $\text{InAs}_{0.32}\text{Sb}_{0.68}$  was found to be 6.3464 Å. The Sb composition of sample A2 was 0.6 and the lattice constant of  $\text{InAs}_{0.4}\text{Sb}_{0.6}$  was 6.3068 Å. The Sb composition of sample A3 was 0.84 and the lattice constant of  $\text{InAs}_{0.16}\text{Sb}_{0.84}$  was 6.4099 Å. The diffraction peaks of GaAs, GaSb,  $\text{InAs}_x\text{Sb}_{1-x}$  and  $\text{Al}_{0.2}\text{In}_{0.8}\text{Sb}$  can be clearly observed for samples A1 and A2. In sample A3, only the diffraction peaks of GaAs, GaSb and  $\text{Al}_{0.2}\text{In}_{0.8}\text{Sb}$  can be observed. This is because the  $\text{InAs}_{0.16}\text{Sb}_{0.84}$  lattice constant of sample A3 is close to the lattice constant of  $\text{Al}_{0.2}\text{In}_{0.8}\text{Sb}$  (6.4106 Å), causing their diffraction peaks to overlap.

The crystalline quality of the epitaxial layers was further assessed by XRD RSM measurements. Figure 5 (a), (b) and (c) show the logarithmic XRD RSM for the symmetrical (004) for sample A1, sample A2 and sample A3, respectively. Apart from the GaAs substrate peak denoted by S, three epitaxial peaks were also identified from Fig. 5 (a), (b) and (c) denoted by L1, L2 and L3, respectively. L1 represents the epitaxial peak of GaSb, L2 represents the epitaxial peak of  $\text{InAs}_x\text{Sb}_{1-x}$  and L3 represents the epitaxial peak of  $\text{Al}_{0.2}\text{In}_{0.8}\text{Sb}$ . Corre-

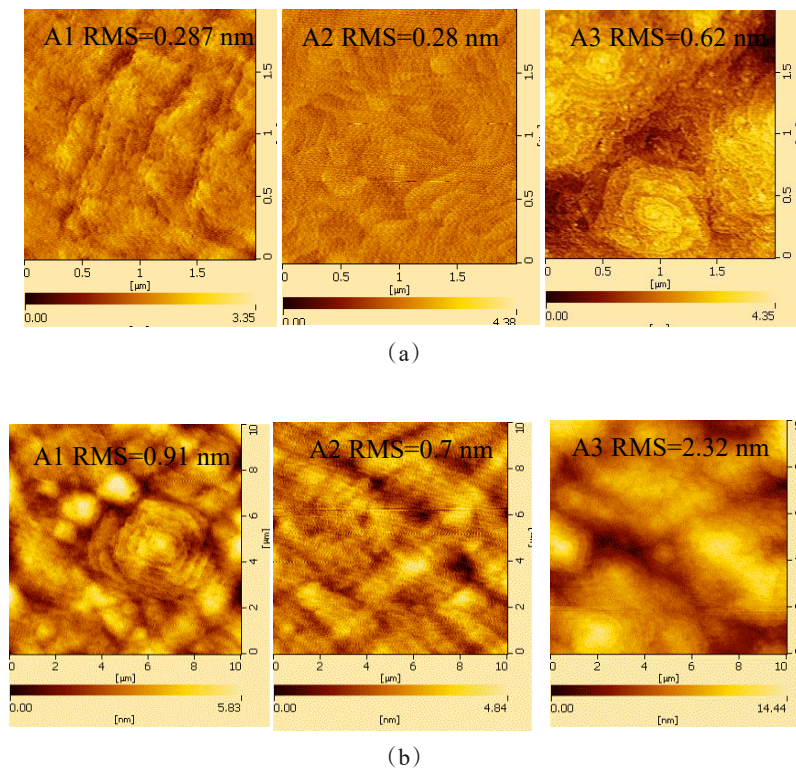


Fig.3 (a)  $2 \times 2 \mu\text{m}^2$  AFM image of samples A1, A2, A3; (b)  $10 \times 10 \mu\text{m}^2$  AFM image of samples A1, A2, A3  
图3 (a)样品 A1、A2、A3 的  $2 \times 2 \mu\text{m}^2$  AFM 扫描图像; (b) 样品 A1、A2、A3 的  $10 \times 10 \mu\text{m}^2$  AFM 扫描图像

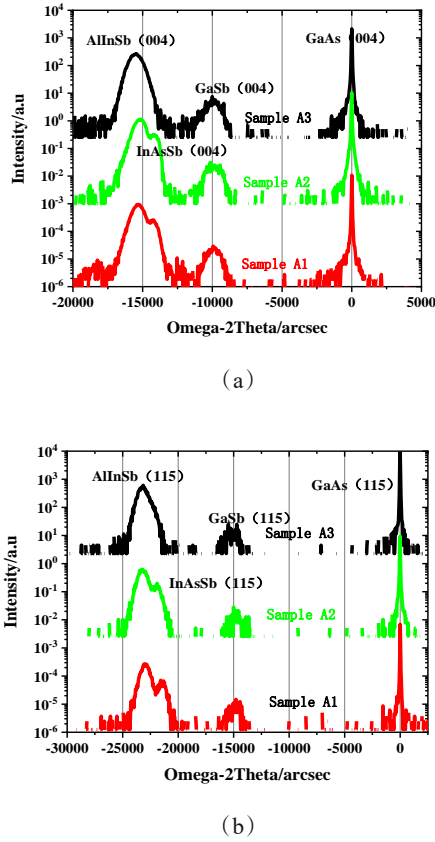


Fig. 4 HRXRD scanning curves of (a) (004) peak and (b) (115) peak for various samples.

图4 样品的HRXRD:(a)(004)扫描和(b)(115)扫描

Table 1 Results calculated from HRXRD measurements  
表1 HRXRD 测量计算结果

Sample	(004)scanning		(115)scanning		a( $\text{\AA}$ )	1-X
	Bragg angle	a $\perp$ ( $\text{\AA}$ )	Bragg angle	a//( $\text{\AA}$ )		
A1	29.06 $^\circ$	6.3435	39.08 $^\circ$	6.3491	6.3464	0.68
A2	29.08 $^\circ$	6.3395	39.62 $^\circ$	6.2765	6.3068	0.6
A3	28.73 $^\circ$	6.41	38.64 $^\circ$	6.4099	6.4099	0.84

sponding to the analysis in Fig. 4, it can be seen that the epitaxial peak of  $\text{InAs}_{0.16}\text{Sb}_{0.84}$  in sample A3 is indeed close to the epitaxial peak of  $\text{Al}_{0.2}\text{In}_{0.8}\text{Sb}$ .

The influence of the V/III ratio on the electrical

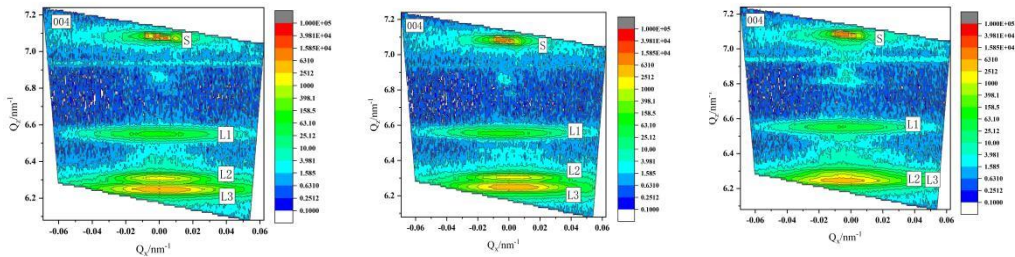


Fig. 5 XRD RSMs of the symmetrical (004) (a) sample A1; (b) sample A2 and (c) sample A3  
图5 对称扫描(004)(a)样品A1;(b)样品A2和(c)样品A3的XRD-RSM

properties of  $\text{InAs}_x\text{Sb}_{1-x}$  thin films was examined by determining the Hall properties. The electron mobility  $\mu$  refers to the average speed of electron units under the electric field intensity. The value of  $\mu$  can be obtained from the following formula:

$$\mu = q < \tau > / m^* \quad (1)$$

where  $m^*$  represents the electron effective mass,  $\tau$  represents the mean free time of electrons and  $q$  represents electron charge.  $\text{InAs}_x\text{Sb}_{1-x}$  is a compound of InSb and InAs materials, so its crystal structure is relatively stable. The room temperature electron effective mass of  $\text{InAs}_x\text{Sb}_{1-x}$  is  $0.023-0.039(1-x)+0.03(1-x)^2 m_0$ . Therefore,  $\text{InAsSb}$  with a 60% Sb component has the lowest electron effective mass among III-V compound semiconductors, resulting in the highest electron mobility<sup>[22,23]</sup>. As shown in Fig. 6, Hall measurements were performed on  $1\text{ cm} \times 1\text{ cm}$  sample pieces at 300 K to obtain the electron mobility, results of  $24\,540\text{ cm}^2/\text{V}\cdot\text{s}$  were obtained for sample A1,  $28\,560\text{ cm}^2/\text{V}\cdot\text{s}$  for sample A2 and  $25\,850\text{ cm}^2/\text{V}\cdot\text{s}$  for sample A3. It can be seen from the above results that the highest mobility is indeed obtained when the Sb component is 0.6. The results of electron mobility in this paper are much better than previously reported, as shown in Table 2. For comparison with the literature, the density of 2DEG concentration was converted into a volume density value of  $1.01 \times 10^{18}\text{ cm}^{-3}$ .

## 2.2 The influences of Sb/In ratios on $\text{Al}_{0.2}\text{In}_{0.8}\text{Sb}/\text{InAs}_x\text{Sb}_{1-x}$ quantum well heterostructures

Although InAsSb has excellent transmission properties, the lack of matching high-quality semi-insulating substrates limits its development. Therefore, an  $\text{Al}_{0.2}\text{In}_{0.8}\text{Sb}$  strain buffer layer was used to release the stress caused by the lattice mismatch between InAsSb and GaAs substrates. The AFM images of  $\text{Al}_{0.2}\text{In}_{0.8}\text{Sb}/\text{InAs}_x\text{Sb}_{1-x}$  quantum well heterostructures grown under different Sb/In ratios are shown in Fig. 7. It showed a  $10 \times 10\ \mu\text{m}^2$  AFM images of sample B1, B2 and B3 with an RMS roughness of 2.794 nm, 1.725 nm and 3.359 nm, respectively. It can be seen that when the Sb/In ratio was 6, the surface of the sample was the smoothest and with its RMS roughness at the lowest of the batch of samples.

The (004) HRXRD scanning curves of samples with different Sb components are shown in Fig. 8. The diffraction intensity of the  $\text{InAs}_x\text{Sb}_{1-x}$  channel layer is very weak because its thickness is too thin. From Fig. 8, it can be observed that the Bragg angles of  $\text{Al}_{0.2}\text{In}_{0.8}\text{Sb}$  in all

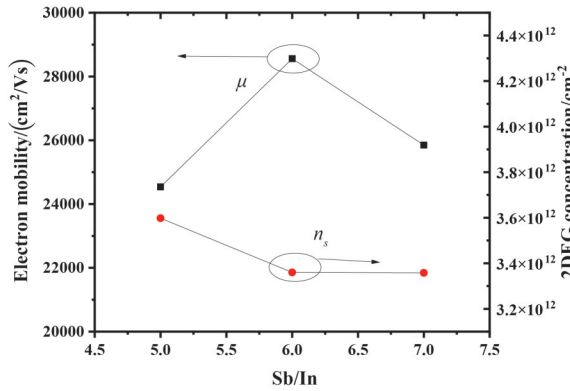


Fig. 6 Electron mobility  $\mu$  and 2DEG concentrations  $n_s$  versus different Sb/In ratios for samples A1, A2, A3

图6 样品A1, A2和A3的电子迁移率和二维电子气浓度与不同的Sb/In比

Table 2 Summary of literature data about the structural properties of  $\text{InAs}_x\text{Sb}_{1-x}$  thin films.

表2  $\text{InAs}_x\text{Sb}_{1-x}$  薄膜结构特性的文献数据汇总

Ref	Sb composition	Thickness (nm)	RMS roughness (nm)	Electron mobility ( $\text{cm}^2/\text{V}\cdot\text{s}$ )	2DEG concentrations ( $\text{cm}^{-3}$ )
21	0.58	1 500	1.9( $10 \times 10 \mu\text{m}^2$ )	-	-
24	0.13	5 000	-	25 000	$5 \times 10^{16}$
25	0.05	800	3.954( $2 \times 2 \mu\text{m}^2$ )	5 430	$1.01 \times 10^{17}$
26	0.9	1 000	1.99( $10 \times 10 \mu\text{m}^2$ )	13 000	$1.3 \times 10^{17}$
This work	0.6	200	0.7( $10 \times 10 \mu\text{m}^2$ )	28 560	$1.01 \times 10^{18}$

samples are the same, indicating that the Al composition is the same. Additionally, it was assumed that the contribution of FWHM mainly comes from lattice distortion caused by dislocations, and the dislocation density in  $\text{Al}_{0.2}\text{In}_{0.8}\text{Sb}$  thin film samples can be calculated based on FWHM. The FWHM of the  $\text{Al}_{0.2}\text{In}_{0.8}\text{Sb}$  buffer layer in samples B1, B2, and B3 are 1 109 arcsec, 997 arcsec, and 1 033 arcsec, respectively, indicating that the quality of the three samples is equivalent.

As shown in Fig. 9, the electron mobilities of samples B1, B2 and B3 at 300 K are  $17\,500 \text{ cm}^2/\text{V}\cdot\text{s}$ ,  $18\,500 \text{ cm}^2/\text{V}\cdot\text{s}$  and  $17\,700 \text{ cm}^2/\text{V}\cdot\text{s}$ , respectively. According to the calculation results in Table 1, the channel materials of samples B1, B2, and B3 are  $\text{InAs}_{0.32}\text{Sb}_{0.68}$ ,

$\text{InAs}_{0.4}\text{Sb}_{0.6}$  and  $\text{InAs}_{0.16}\text{Sb}_{0.84}$ , respectively. Figure 9 shows that the  $\text{Al}_{0.2}\text{In}_{0.8}\text{Sb}/\text{InAs}_x\text{Sb}_{1-x}$  quantum well heterostructures obtain the maximum electron mobility when the Sb component is 0.6. This result is consistent with the Hall test results in Table 1. This is because the effective mass of electrons reaches a minimum value when the Sb component is 60%. The 2DEG concentrations in the channel are  $9.44 \times 10^{11} \text{ cm}^{-2}$ ,  $1 \times 10^{12} \text{ cm}^{-2}$  and  $7.89 \times 10^{11} \text{ cm}^{-2}$  respectively, with little change.

### 2.3 The influences of As/In ratio on $\text{Al}_{0.2}\text{In}_{0.8}\text{Sb}/\text{InAs}_x\text{Sb}_{1-x}$ quantum well heterostructures

It can be observed from the comparison between Fig. 6 and Fig. 9 that the electron mobility of sample A2 in  $\text{InAs}_x\text{Sb}_{1-x}$  with 15 nm thickness was significantly lower. Therefore, three samples with different As/In ratios were grown for study after changing the channel thickness in the quantum well from 15 nm to 30 nm. Figure 10 displays the images of a  $10 \mu\text{m} \times 10 \mu\text{m}$  surface scan of samples C1, C2 and C3 with an RMS roughness of 1.757 nm, 1.785 nm and 0.68 nm, respectively. It shows that sample C3 has a smoother surface than other samples.

The (004) HRXRD scanning curves of samples with different As components are shown in Fig. 11. In Fig. 11, there are only three peaks corresponding to the GaAs substrate, GaSb buffer layer, and  $\text{Al}_{0.2}\text{In}_{0.8}\text{Sb}$  strain buffer layer. Because the thickness of the channel layer  $\text{InAs}_x\text{Sb}_{1-x}$  was too thin to be observed. The peaks of the  $\text{Al}_{0.2}\text{In}_{0.8}\text{Sb}$  strain buffer layer in all samples are clearly visible. The FWHM of samples C1, C2 and C3 are 903 arcsec, 936 arcsec, and 986 arcsec, respectively. The similar FWHM and Bragg peak positions indicate that the crystalline quality of all samples is similar.

Electron mobility is an important electrical parameter that can be used to evaluate whether  $\text{Al}_{0.2}\text{In}_{0.8}\text{Sb}/\text{InAs}_x\text{Sb}_{1-x}$  quantum well heterostructures grown by MBE can be used to prepare high mobility transistors. As shown in Fig. 12, the electron mobility of samples C1, C2, and C3 at 300 K is  $10\,100 \text{ cm}^2/\text{V}\cdot\text{s}$ ,  $22\,020 \text{ cm}^2/\text{V}\cdot\text{s}$  and  $28\,300 \text{ cm}^2/\text{V}\cdot\text{s}$ , respectively. Because In atoms will occupy a portion of As and Sb atomic positions as well as interstitial positions in the lattice at the lower V/III flux ratio, this can easily cause In atom clusters. This situation will cause a decrease in the electron mobility as seen for samples C1 and C2.

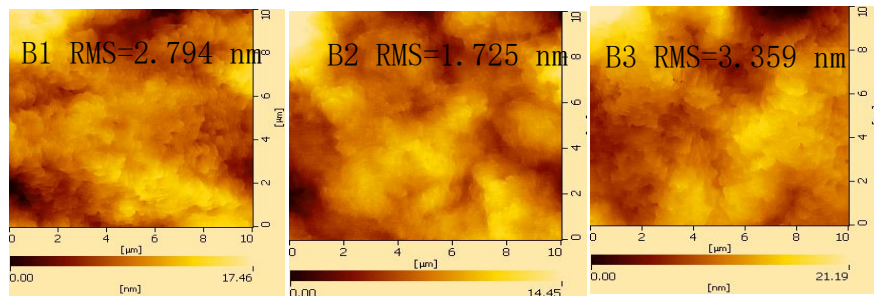


Fig. 7  $10 \times 10 \mu\text{m}^2$  AFM image of samples B1, B2, B3

图7 样品B1, B2, B3的 $10 \times 10 \mu\text{m}^2$  AFM扫描图像

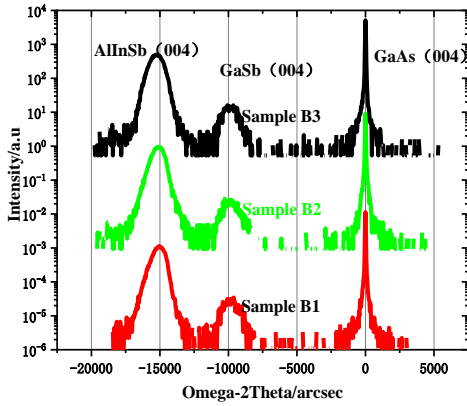


Fig. 8 HRXRD scanning curves of (004) peak for samples B1, B2, B3

图8 样品B1、B2、B3的(004)峰HRXRD扫描曲线

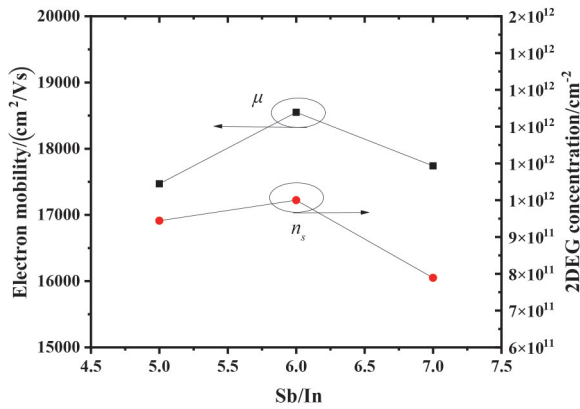


Fig. 9 Electron mobility  $\mu$  and 2DEG concentrations  $n_s$  versus different Sb/In ratios

图9 电子迁移率 $\mu$ 和2DEG浓度 $n_s$ 与不同Sb/In比的关系

#### 2.4 The influences of channel thickness on $\text{Al}_{0.2}\text{In}_{0.8}\text{Sb}/\text{InAs}_{0.4}\text{Sb}_{0.6}$ quantum well heterostructures

Based on the previous optimization results, it was found that the thickness of the  $\text{InAs}_x\text{Sb}_{1-x}$  layer has a significant impact on electron mobility. Therefore, the influence of channel thickness on electron mobility and 2DEG concentration was studied while fixing the Sb/In ra-

tio to 6 and As/In ratio at 3. Figure 13 shows the electron mobility and 2DEG concentration dependence on channel thickness at 300 K. It is evident that the electron mobility of samples increases quickly from 18 500  $\text{cm}^2/\text{Vs}$  to 28 300  $\text{cm}^2/\text{Vs}$  with the increase of the channel width from 15 nm to 30 nm. When the  $\text{InAs}_{0.4}\text{Sb}_{0.6}$  channel width is 30 nm, the mobility reaches the maximum of 28 300  $\text{cm}^2/\text{Vs}$ . When the channel width is larger than 30 nm, the electron mobility decreases slowly from 28 300  $\text{cm}^2/\text{Vs}$  to 27 400  $\text{cm}^2/\text{Vs}$ . Interface roughness scattering is the main factor limiting the mobility in  $\text{InAs}_{0.4}\text{Sb}_{0.6}$  channels thinner than 30 nm, while dislocation scattering is the main factor limiting the mobility in  $\text{InAs}_{0.4}\text{Sb}_{0.6}$  channels above 30 nm. Therefore, the electron mobility is no longer increasing with channel layer thickness after 30 nm. After our literature search, the highest electron mobility reported for the  $\text{InAsSb}$  quantum well heterostructures is currently 28 000  $\text{cm}^2/\text{Vs}$ <sup>[27]</sup>. They used a digital alloy method to grow  $\text{InAs}_{0.125}\text{Sb}_{0.875}$  material as the channel layer. However, this method of growing  $\text{InAs}_{0.125}\text{Sb}_{0.875}$  channel layers using digital alloys introduces more interfaces. Moreover, interface roughness scattering will have a significant impact on electron mobility. Therefore, the results obtained by the growth method used in this article have obvious advantages. From Fig. 13, it can be seen that the 2DEG in the quantum well is  $6.03 \times 10^{11} - 1.01 \times 10^{12} \text{ cm}^{-2}$ . The overall trend change is not significant.

### 3 Conclusion

In summary, the influence of the V/III ratio on the transport properties and crystal quality of the 200 nm  $\text{InAs}_x\text{Sb}_{1-x}$  thin film and  $\text{Al}_{0.2}\text{In}_{0.8}\text{Sb}/\text{InAs}_x\text{Sb}_{1-x}$  quantum well heterostructures has been investigated. The calculation results indicated that the Sb component is 0.6 in the  $\text{InAs}_x\text{Sb}_{1-x}$  thin film when grown under the conditions of Sb/in ratio of 6 and As/in ratio of 3. Meanwhile, the highest electron mobility of  $\text{InAs}_x\text{Sb}_{1-x}$  thin film measured at room temperature was 28 560  $\text{cm}^2/\text{V} \cdot \text{s}$ . In addition, the highest electron mobility of the  $\text{Al}_{0.2}\text{In}_{0.8}\text{Sb}/\text{InAs}_{0.4}\text{Sb}_{0.6}$  quantum well heterostructures was obtained at 28 300  $\text{cm}^2/\text{V} \cdot \text{s}$  for a sample with a channel thickness of 30 nm grown under the conditions where Sb/in ratio was 6 and As/in ratio was 3. This investigation reports the high-quality film and high electron mobility obtained for  $\text{Al}_{0.2}\text{In}_{0.8}\text{Sb}/$

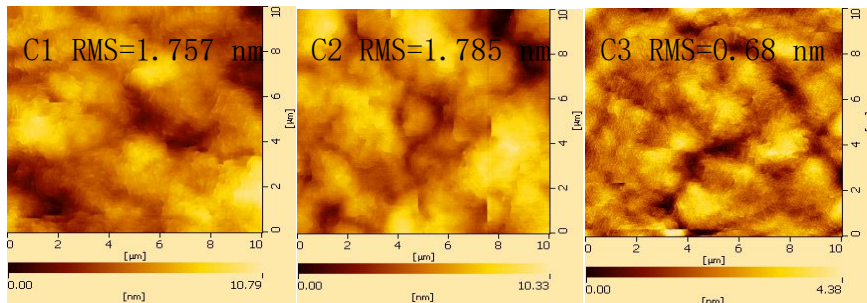


Fig. 10  $10 \times 10 \mu\text{m}^2$  AFM image of samples C1, C2, C3

图10 样品C1、C2、C3的 $10 \times 10 \mu\text{m}^2$  AFM图像

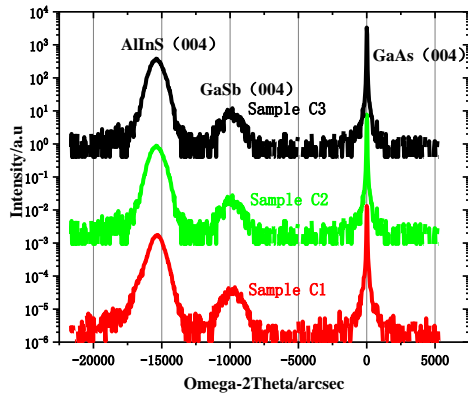


Fig. 11 HRXRD scanning curves of (004) peak for samples C1, C2, C3

图 11 样品 C1、C2、C3 的 (004) 峰 HRXRD 扫描曲线

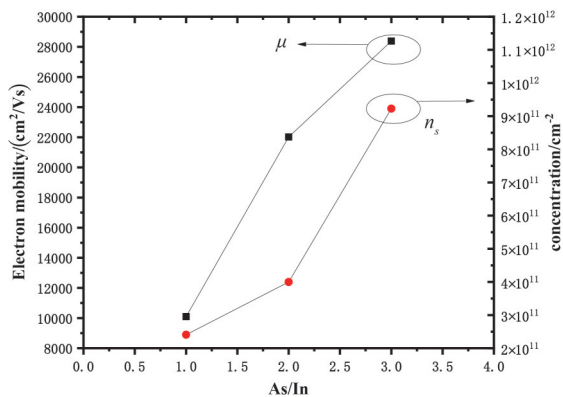


Fig. 12 Electron mobility  $\mu$  and 2DEG concentrations  $n_s$  versus different As/In ratios

图 12 电子迁移率  $\mu$  和 2DEG 浓度  $n_s$  与不同 As/In 比的关系

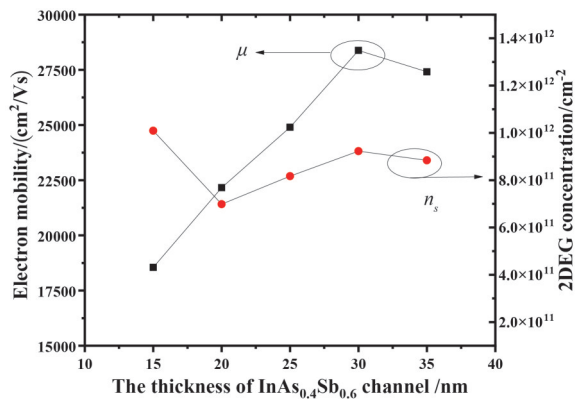


Fig. 13 Electron mobility  $\mu$  and 2DEG concentration  $n_s$  versus different channel thickness

图 13 电子迁移率  $\mu$  和 2DEG 浓度  $n_s$  与不同沟道厚度的关系

$\text{InAs}_{0.4}\text{Sb}_{0.6}$  heterostructures lattice-matched to GaAs and opens the exploration of their uses in high electron mobility transistors.

## References

- [1] Shandilya S, Madhu C, Kumar V. Performance Analysis of the Gate All Around Nanowire FET with Group III-V Compound Channel Materials and High-k Gate Oxides[J]. *Transactions on Electrical and Electronic Materials*, 2023, **24**(3):228-234.
- [2] Hoshi T, Kashio N, Shiratori Y, *et al.* InGaP/GaAsSb/InGaAsSb double heterojunction bipolar transistors with 703-GHz  $f_{\text{max}}$  and 5.4-V breakdown voltage[J]. *IEICE Electronics Express*, 2019.
- [3] Le S P, Suzuki T K. Electron mobility anisotropy in InAs/GaAs(001) heterostructures [J]. *Applied Physics Letters*, 2021, **118** (18) : 182101.
- [4] Komatsu S, Irie H, Akiho T, *et al.* Gate tuning of fractional quantum Hall states in an InAs two-dimensional electron gas [J]. *Physical Review B*, 2021.
- [5] Menon H, Morgan N P, Hetherington C, *et al.* Fabrication of Single-Crystalline InSb-on-Insulator by Rapid Melt Growth [J]. *Physica status solidi, A. Applications and materials science ePSS*, 2022 (4):219.
- [6] Lei Z, Cheah E, Rubi K, *et al.* High-quality Two-Dimensional Electron Gas in Undoped InSb Quantum Wells [J]. 2021.
- [7] Svensson S P, Beck W A, Sarney W L, *et al.* Temperature dependent Hall effect in InAsSb with a 0.11 eV 77 K-bandgap [J]. *Applied Physics Letters*, 2019, **114** (12) :122102.
- [8] Wei Q, Wang H, Zhao X, *et al.* Electron mobility anisotropy in (Al, Ga) Sb/InAs two-dimensional electron gases epitaxied on GaAs (001) substrates [J]. *Journal of Semiconductors* 43.7(2022) :6.
- [9] Chen Y, Lin H, Lee K, *et al.* Inverted-Type InAlAs/InAs High-Electron-Mobility Transistor with Liquid Phase Oxidized InAlAs as Gate Insulator. [J]. *Materials (Basel, Switzerland)*, 2021, **14**(4):970.
- [10] Sukhanov M A, Bakarov A K, Zhuravlev K S. AlSb/InAs Heterostructures for Microwave Transistors [J]. *Technical Physics Letters: Letters to the Russian Journal of Applied Physics*, 2021, **47** (2) : 139-142.
- [11] Bergeron E A, Sfigakis F, Shi Y, *et al.* Field effect two-dimensional electron gases in modulation-doped InSb surface quantum wells [J]. *Applied Physics Letters*, 2023, **122**(1):012103.
- [12] Kumar V A, Anandan P. Analysis & Simulation of InSb HEMT Device for Low Power and Switching Applications [J]. 2015, **7**:79-81.
- [13] Boland J L, Amaduzzi F, Sterzl S, *et al.* High Electron Mobility and Insights into Temperature-Dependent Scattering Mechanisms in InAsSb Nanowires. [J]. *Nano Letters*, 2018, **18**(6):3703 - 3710.
- [14] Kruppa W, Boos J B, Bennett B R, *et al.* Low-frequency noise characteristics of AlSb/InAsSb HEMTs [J]. *Solid State Electronics*, 2004, **48**(10/11):2079-2084.
- [15] Zhang Y, Zhang Y, Guan M, *et al.* Theoretical study of transport property in InAsSb quantum well heterostructures [J]. *Journal of Applied Physics*, 2013, **114** (15) :111108-1.
- [16] Devakadaksham G, Kumar M, Sarkar C K. Threading dislocation degradation of InSb to InAsSb subchannel double heterostructures [J]. *Electronic Materials Letters*, 2015, **11**(4):1-6.
- [17] Zhang Y, Zhang Y, Wang C, *et al.* Transport properties in AlInSb/InAsSb heterostructures [J]. *Journal of Applied Physics*, 2013, **114** (24):243710.
- [18] Egan R J, Chin V W L, Tansley T L. Dislocation scattering effects on electron mobility in InAsSb [J]. *Journal of Applied Physics*, 1994, **75**(5):2473-2476.
- [19] Mahadik N, Svensson S. Dislocation analysis of epitaxial InAsSb on a metamorphic graded layer using x-ray topography [J]. *Journal of Applied Physics*, 2022, **131** (18), 184501.
- [20] Taghipour Z, Liu A W K, Fastenau J M, *et al.* Investigation of bulk and surface minority carrier lifetimes in metamorphic InAsSb grown on GaAs and Si [J]. *Journal of Applied Physics*, 2021, **129** (1) : 015106.
- [21] Woo S, Yeon E, Chu R J, *et al.* Metamorphic growth of 0.1 eV InAsSb on InAs/GaAs virtual substrate for LWIR applications [J]. *Applied Surface Science: A Journal Devoted to the Properties of Interfaces in Relation to the Synthesis and Behaviour of Materials*, 2023 (Jun. 30) :623:156899.
- [22] Manyk T, Rutkowski J, Kopytko M, *et al.* Determination of the Strain Influence on the InAs/InAsSb Type-II Superlattice Effective Masses [J]. *Sensors (Basel, Switzerland)*, 2022, **22**(21), 8243.
- [23] El Khalidi Z, Grein C H, Ciani A, *et al.* Assessing Sb Cross Incorporation in InAs/InAsSb Superlattices [J]. *Journal of Electronic Materials*, 2022, **51**(12):6784-6791.

- [24] Benyahia D, Kubiszyn L, Michalczewski K, *et al.* Investigation on the InAs<sub>1-x</sub>Sb<sub>x</sub> epilayers growth on GaAs (001) substrate by molecular beam epitaxy[J]. *Journal of Semiconductors*, 2018, **39**(03):18-22.
- [25] Ni P N, Tong J C, Tobing L Y M, *et al.* A buffer-free method for growth of InAsSb films on GaAs (001) substrates using MOCVD[J]. *Journal of Crystal Growth*, 2016;S0022024816308442.
- [26] Gao H, Wang W, Jiang Z, *et al.* The growth parameter influence on the crystal quality of InAsSb grown on GaAs by molecular beam epitaxy[J]. *Journal of Crystal Growth*, 2007, **308**(2):406-411.
- [27] Kudo M, Mishima T, Tanaka T. Increased electron mobility of InAsSb channel heterostructures grown on GaAs substrates by molecular beam epitaxy [J]. *Journal of Vacuum Science & Technology. B*, 2000, **18**(2):746-750.